ARTICLE

Morphology and Growth Process of Bat-like ZnO Crystals by Thermal Evaporation

Pin Gao, Kai Wang, Chao Huang, Lu Meng, Fa-qiang Xu*

National Synchrotron Radiation Laboratory, University of Science and Technology of China, Hefei 230026, China

(Dated: Received on December 22, 2015; Accepted on February 25, 2016)

A novel bat-like ZnO nanostructure was synthesized on the silicon substrate by simple thermal evaporation of zinc powders without any catalyst. Each bat-like nanorod ("nanobat") is composed of a hexagonal head, a continuous neck and a thin handle. High-resolution transmission electron microscopy and selected area electron diffraction results reveal the single-crystalline feature and the growing direction along [0001] of the nanobat. The vapor-solid mechanism was found suitable to explain the growth process of the nanobat and a schematic model was proposed in detail based on the experimental results.

Key words: ZnO, Thermal evaporation, Nanostructure, Growth process

I. INTRODUCTION

ZnO, with a wide band gap (3.37 eV) and high exciton binding energy (∼60 meV), has drawn great interest as a promising material for solar cells [1], gas sensors [2], ultraviolet photoresistors [3], and nanolight filter devices [4]. Many groups proposed that grain size, crystal structure, and surface morphology could significantly influence the optical, electrical and other properties, so considerable efforts have been devoted to the synthesis of various ZnO nanostructures. For example, Wu *et al*. demonstrated that ZnO nanostructures grown on different buffer layers exhibited different crystalline qualities, and optical properties, and it was proposed that stresses and threading dislocations between ZnO films and substrates could be released and reduced by different buffer layers to different degrees [5]. Lv *et al*. investigated the effect of solution concentration on microstructure, surface morphology and optical band gap of ZnO thin films by hydrothermal method, also prepared a typical tower-like ZnO thin film composed of many ZnO nanosheets from 0.08 mol/L solution [6]. Gao *et al*. reported that ZnO bicrystalline nanosheets with twin defects could be synthesized with Ag_xAu_{1-x} alloy catalyst which could lower the formation energy of the twinning defect of wurtzite ZnO [7]. Besides the common ZnO nanomaterials, more and more complex and advanced nanostructures, such as sea-urchin shaped ZnO [4] and tetrapod-like ZnO nanocrystals [8], have been fabricated and extensively studied because they can be directly utilized as building blocks in construction of nanoelectronics and photonics due to their single-crystalline feature, superior optical, and mechanical properties.

Numerous methods have been carried out in synthesizing ZnO nanostructures, including thermal evaporation [9], chemical vapor deposition method [10], hydrothermal method [11], catalyst-assisted vapor-phase transport [12], metal-organic vapor-phase epitaxy [13], electrochemical process [14], and porous template method [15], *etc*. However, most of the methods have drawbacks more or less. Exotic metal catalysts which affect the optical and electrical properties to restrict the application in electronics and photonics can be easily brought into the products by catalyst-assisted vapor-phase transport method; as to porous template method, the templates are usually toxic and the processes are complicated. Compared with these methods, thermal evaporation of zinc powders is a facile, flexible and pure-crystalline method, which has been widely used in synthesizing various morphologies. For example, wurtzite ZnO nanonail structures have been fabricated on sapphire by thermal evaporation of Zn powders in oxygen ambient as reported by Kumar *et al*. [16]; a crown-like ZnO crystal composed of a hexagonal cap and a tower-like shaft was synthesized on silicon wafer by Zhu *et al*. [17].

In this work, we have fabricated a peculiar bat-like ZnO nanostructure with valuable application as building blocks in construction of nanoelectronics and photonics by thermal evaporation of zinc powders in a common furnace, with no catalysts and carrier gases. Furthermore, our results supply more insight into the growth mechanism and the detailed growth process of the complicated bat-like nanostructures based on the morphology characteristic and structural analysis.

*Author to whom correspondence should be addressed. E-mail: fqxu@ustc.edu.cn, Tel: +86-551-63602127

 ©2016 Chinese Physical Society

II. EXPERIMENTS

The bat-like ZnO nanostructures were synthesized by a simple thermal evaporation approach in a furnace equipped with a quartz tube. About 5.0 g zinc powders (99.999%) were placed in a ceramic boat which was transferred into the center of the furnace tube. The Si substrate which had been cleaned by sonication in ethanol was placed just beside the boat. The quartz tube was open to the air at both ends ensuring that enough oxygen could be provided. The temperature of the furnace was increased to 650 °C with a constant rate of 35 °C/min, and then remained for 120 min. After termination of the reaction, the furnace was cooled to room temperature naturally, and the products were condensed on the surface of Si substrate. The morphologies of the ZnO nanostructures were characterized by field-emission scanning electron microscopy (FESEM, JEOL JSM-6700F). The microstructure information was characterized with transmission electron microscopy (TEM, JEOL-2000) operated at 200 kV.

III. RESULTS AND DISCUSSION

Figure 1 shows the SEM image of the ZnO nanostructures as prepared sample. Obviously each individual structure looks like a bat of baseball which is composed of a thin handle and a thick head with clear hexagonal feature. From the point of crystallography, for the wurtzite hexagonal crystal structure, ZnO crystal tends to thermodynamically form faceted hexagonal structure which have {0001} as top and bottom surfaces enclosed by six crystallographic equivalent $\{01\bar{1}0\}$ or $\{21\bar{1}0\}$ side surfaces, due to the low energy facets of {0001}, $\{01\bar{1}0\}$, and $\{21\bar{1}0\}$ [18]. So the heads of the nanobats have a tendency to be hexagonally-shaped. The diameters of the heads are 1−2 mm, and that of the handles are in the range of 100−300 nm. The lengths of the nanobats are several micrometers. Some nanobats are dispersed on the substrate individually, while most of the nanobats assemble together with handles jointing.

The structure of the nanobat was further analyzed by high magnification TEM. As Fig.2 illustrates, the bat-like structure is perfectly reserved although it suffered from the ultrasonic treatment in the TEM sample preparation. The inset selected area electron diffraction (SAED) pattern shows that the nanobat possesses single-crystalline feature, with no defects or dislocations, and also exhibits a [0001] preferred orientation.

It is worth mentioning that a bottleneck phenomenon is visible in the middle of each nanobat. Figure 3 illustrates the high magnification TEM (inset) image and the corresponding partial high-resolution transmission electron microscopy (HRTEM) image of the bottleneck of the ZnO nanobat, respectively. The clear lattice fringes further prove that the ZnO nanobat has the nature of single crystal. The lattice interspacing is estimated to be about 0.26 nm consistent with that of the hexagonal wurtzite ZnO structure along [0001] direction, which confirms that the growth direction of the nanobat is along [0001] *c*-axis.

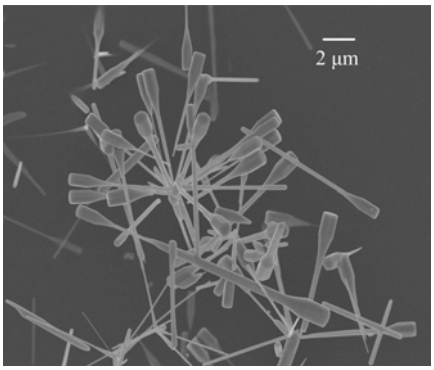

FIG. 1 SEM image of the bat-like ZnO nanostructures.

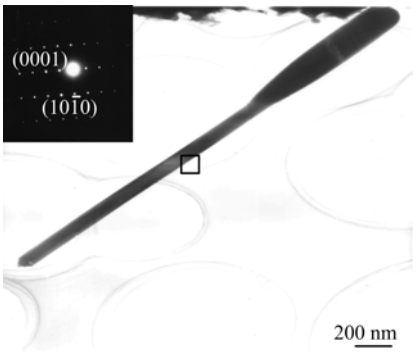

FIG. 2 High magnification TEM image of a ZnO nanobat, with the corresponding SAED pattern in the inset.

Apparently, the edge of the bottleneck is found to be step type along with [0001] direction, as shown in Fig.3. This phenomenon has implication for the detailed growth process for ZnO nanobats. Since no metal catalyst is introduced during the experiment, the vapor-liquid-solid mechanism [19] is not suitable for our system. Moreover, the ZnO nanobats show high crystallinity, so screw-dislocation evolved growth mechanism [20] which is characterized by the presence of an axial dislocation in growth of crystal whiskers, is not relevant to our results either. We infer that the growth mode of the nanobat showing the phenomenon of step type is related to the traditional vapor-solid (VS) growth mechanism [21].

In terms of VS mechanism, the crystal growth process is generally divided into two stages: nucleation and growth. For the case of the ZnO nanobat, in the first stage, Lao *et al*. proposed that zinc powders were heated to generate Zn vapors and reacted with O_2 in the furnace, then the resultant ZnO solid or ZnO_x (x<1) or liquid Zn metal droplets condensed on the low temperature Si substrate and acted as nucleation centers [22]. After initial nucleation, each nanobat can be formed

DOI:10.1063/1674-0068/29/cjcp1512258 ©2016 Chinese Physical Society

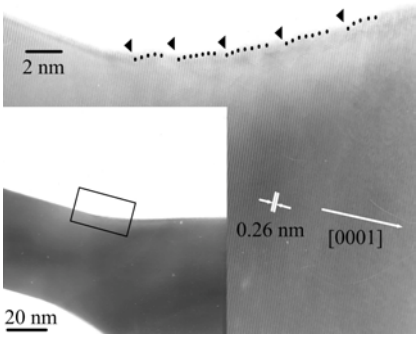

FIG. 3 TEM image (inset) and HRTEM image of the bottleneck of the ZnO nanobat.

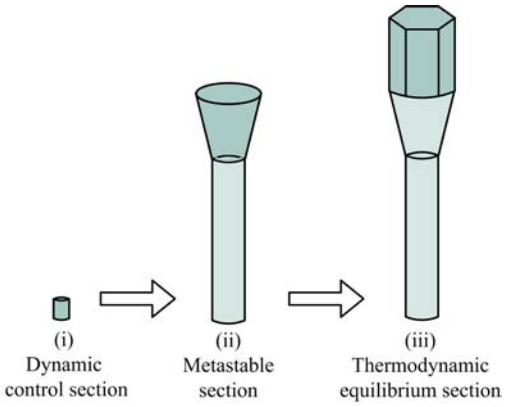

FIG. 4 Schematic diagram for the growth process of a ZnO nanobat.

through three sequential growth sections: (i) the dynamic control section, (ii) the metastable section, and (iii) the thermodynamic equilibrium section. As is well known to all, the morphology of ZnO crystals may be influenced by saturated vapor pressure, just as Gong *et al.* inferred [23]. In the present experiment, the oxygen pressure was approximately constant due to the open quartz tube, while the partial pressure of Zn vapor changed from less to more with the increase of temperature and finally kept stable at the fixed temperature of 650 °C. During the initial reaction section, only low concentration of Zn vapor could be provided because the zinc powders were not evaporated enough. The low supersaturation level was preferred for longitudinal growth [24], thus, a thin ZnO nanorod with large length-diameter ratio was formed which would act as the handle in the coming nanobat. It was an unstable section where the system was controlled by reaction dynamics. As the concentration of Zn vapor increased gradually to a critical level, the nanorod started to grow along both the transverse direction and longitudinal one [25], leading to the formation of the neck of the nanobat. It was a metastable section and wouldn't stop until the system gradually found an equilibrium status. Therefore, the change of the neck from the handle to the head was not abrupt. After the concentration of Zn vapor reached a high and stable level, a thermodynamic equilibrium was attained, and the nanorod began to elongate along [0001] with an uniform diameter due to the stable atmosphere of ZnO_x reactant vapor absorbed by the top of the nanorods [25], which produced the head of the nanobat. And as shown in Fig.1, the cross section of the nanohead appeared to be hexagonal, consistent with the ZnO hexagon crystal structure [18], which implies that the nanorod has perfect crystal quality. In order to better understand the growth behavior of the ZnO nanobat, a schematic diagram of the growth process is proposed and illustrated in Fig.4.

Besides the single nanobat structure, some nanobats assembled together with handles jointing as shown in Fig.1. Similar junctions connected by heads have been reported in several literatures, it was usually proposed that the growing process of an individual nanostructure was from head to tip as the example of tetrapod-like ZnO structure [8, 26]. With respect to the tetrapod-like structure, the "octa-twin" nucleus [27], composing of four positively charged (0001) surfaces and four negatively charged $(000\bar{1})$ surfaces, was recognized as the key element for the formation of the tetrapod-like configuration. After the nucleus was formed, the positively charged surfaces preferred to adsorb reactant vapor, leading four hexagonal nanorods to sprout out [28]. And then the octa-twin nucleus cracked in order to release the accumulated misfit strain energy between twin boundaries [29]. Finally, the tetrapod-like ZnO nanostructures were formed. In our work, the amount of branches is not constant, which seems more complicated than tetrapod-like ZnO nanostructures. In order to explain the multi-branch phenomenon, two formation stages of the ZnO branch structures are concluded as follows: firstly, several polyhedron nucleations, assembled by different amounts of particles due to the minimization of surface energies, exposed to vapor with different amounts of active (0001) surfaces; secondly, reactant vapor was adsorbed and deposited on the active (0001) surfaces of polyhedron nucleations continuously. As a result, single or multiple nanobats grew out along preferred [0001] direction from the polyhedron nucleations radically.

Among the branch structures, the three-branch structure shown in Fig.5(a) is the most typical one to interpret the formation of the junction structure. As the HRTEM image demonstrated in Fig.5(b) for the three-branch junction, the atomic level interface between two branches could be observed clearly and showed high crystallinity, without stacking faults or small angle grain boundaries, which indicated the multiply twinned particles feature of the three-branch junction. It can be inferred that the nucleus was assembled by three particles due to minimization of surface energies, and then three branches grew out from the polyhedron nucleation center. The SAED pattern in Fig.5(c) on the

DOI:10.1063/1674-0068/29/cjcp1512258 ©2016 Chinese Physical Society

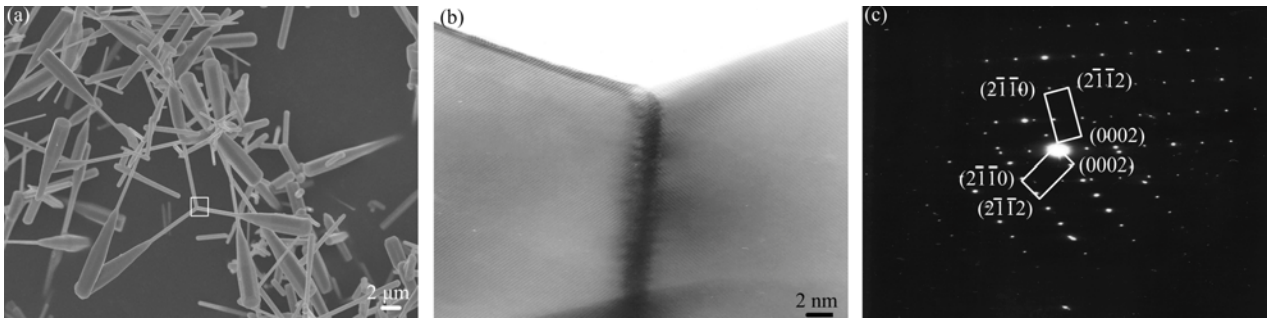

FIG. 5 (a) SEM, (b) HRTEM, and (c) SAED images of the three-branch junction.

three-branch junction illustrated that the microstructures were single-crystalline and the preferred direction was along [0001] direction, consistent with the nanostructure of the single nanobat as mentioned above. Thus, it was proposed that each nanobat underwent a similar three-section growth process after initial polyhedron nucleation. As a conclusion, the nucleation and growth of the three-branch structure can be proposed as shown in Fig.6.

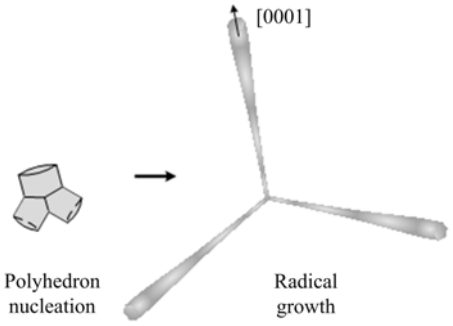

FIG. 6 Schematic diagram of the nucleation and growth of three-branch structure.

IV. CONCLUSION

Bat-like ZnO nanostructures were synthesized on silicon substrate by thermal evaporation of zinc powders in a near ambient atmosphere. The non-metal-catalyst method ensures the high purity of the products. The SEM results show that each nanobat is composed of a hexagonal head, a continuous neck, and a thin handle. The diameters of the heads are 1−2 mm, 100−300 nm of the handles, and the lengths are several micrometers. The SAED and HRTEM results show that the ZnO nanobat is of high crystallinity and grows along [0001] direction. Through HRTEM analysis, three growth sections of a nanobat are summarized: dynamic control section, metastable section and thermodynamic equilibrium section, which can interpret the formation of the ZnO nanobats reasonably. Regarding to the multi-branch junction, it is proposed that the growth process of branch-structure can be summarized into polyhedron nucleation and radical growth. The peculiar bat-like ZnO nanostructures may be a promising candidate for fabricating nanoelectronics and photonics devices.

V. ACKNOWLEDGMENTS

This work is supported by Scientific Research Grant of Hefei Science Center of Chinese Academy of Science (No.2015SRG-HSC032) and the National Natural Science Foundation of China (No.U1232137).

[1] F. Tong, K. Kim, D. Martinez, R. Thapa, A. Ahyi, J. Williams, D. J. Kim, S. Lee, E. Lim, K. K. Lee, and M. Park, Semicond. Sci. Tech. **27**, 105005 (2012).
[2] J. Huang, Y. Wu, C. Gu, M. Zhai, K. Yu, M. Yang, and J. Liu, Sensor. Actuat. B **146**, 206 (2010).
[3] F. J. Liu, Z. F. Hu, J. Sun, Z. J. Li, H. Q. Huang, J. W. Zhao, X. Q. Zhang, and Y. S. Wang, Solid. State. Electron. **68**, 90 (2012).
[4] Y. H. Su and W. Y. Chen, Appl. Phys. Lett. **101**, 133101 (2012).
[5] X. Wu, B. Huang, H. Zhan, and J. Kang, J. Cryst. Growth **318**, 519 (2011).
[6] J. G. Lv, F. J. Shang, G. C. Pan, F. Wang, Z. T. Zhou, C. L. Liu, W. B. Gong, Z. F. Zi, X. S. Chen, G. He, M. Zhang, X. P. Song, Z. Q. Sun, and F. Liu, J. Mater. Sci.: Mater. Electron. **25**, 882 (2014).
[7] Z. W. Gao, Y. Lin, J. W. Li, and X. P. Wang, Chin. J. Chem. Phys. **27**, 350 (2014).
[8] F. Wang, X. Cai, D. Yan, Z. Zhu, and X. Gu, J. Semi. **35**, 063004 (2014).
[9] L. B. Feng, A. H. Liu, M. Liu, Y. Y. Ma, J. Wei, and B. Y. Man, Mater. Charact. **61**, 128 (2010).
[10] B. H. Juarez, P. D. Garcia, D. Golmayo, A. Blanco, and C. Lopez, Adv. Mater. **17**, 2761 (2005).
[11] S. Ohara, T. Mousavand, T. Sasaki, M. Umetsu, T. Naka, and T. Adschiri, J. Mater. Sci. **43**, 2393 (2008).
[12] C. X. Xu, X. W. Sun, Z. L. Dong, and M. B. Yu, J. Cryst. Growth **270**, 498 (2004).
[13] K. Ogata, K. Maejima, Sz. Fujita, and Sg. Fujita, J.

DOI:10.1063/1674-0068/29/cjcp1512258 ©2016 Chinese Physical Society

Cryst. Growth **248**, 25 (2003).
[14] B. Q. Cao, W. P. Cai, G. T. Duan, Y. Li, Q. Zhao, and D. P. Yu, Nanotechnology **16**, 2567 (2005).
[15] J. S. Jie, G. Z. Wang, Q. T. Wang, Y. M. Chen, X. H. Han, X. P. Wang, and J. G. Hou, J. Phys. Chem. B **108**, 11976 (2004).
[16] M. Senthil Kumar, D. Chhikara, and K. M. K. Srivatsa, Cryst. Res. Technol. **46**, 991 (2011).
[17] G. P. Zhu, C. X. Xu, J. Zhu, and M. H. Wang, J. Mater. Sci. **46**, 1877 (2010).
[18] W. J. Li, E. W. Shi, W. Z. Zhong, and Z. W. Yin, J. Cryst. Growth **203**, 186 (1999).
[19] R. S. Wagner and W. C. Ellis, Appl. Phys. Lett. **4**, 89 (1964).
[20] C. M. Drum and J. W. Mitchell, Appl. Phys. Lett. **4**, 164 (1964).
[21] G. W. Sears, Acta. Metall. Sin. **3**, 6 (1955).
[22] J. Y. Lao, J. Y. Huang, D. Z. Wang, and Z. F. Ren, Nano. Lett. **3**, 235 (2003).
[23] W. B. Gong, G. C. Pan, F. J. Shang, F. Wang, Z. T. Zhou, C. L. Liu, M. Zhao, Z. F. Zi, Y. Y. Wei, J. G. Lv, X. S. Chen, G. He, M. Zhang, X. P. Song, and Z. Q. Sun, J. Mater. Sci.: Mater. Electron. **25**, 2948 (2014).
[24] F. Shi and C. S. Xue, CrystEngComm. **14**, 4173 (2012).
[25] J. F. Kong, D. H. Fan, and Y. F. Zhu, Mat. Sci. Semicon. Proc. **15**, 258 (2012).
[26] Y. Zhang, H. B. Jia, X. H. Luo, X. H. Chen, D. P. Yu, and R. M. Wang, J. Phys. Chem. B **107**, 8289 (2003).
[27] S. Takeuchi, H. Iwanaga, and M. Fujii, Philos. Mag. A **69**, 1125 (1994).
[28] W. D. Yu, X. M. Li, and X. D. Gao, J. Cryst. Growth **270**, 92 (2004).
[29] C. Ronning, N. G. Shang, I. Gerhards, H. Hofsass, and M. Seibt, J. Appl. Phys. **98**, 034307 (2005).

DOI:10.1063/1674-0068/29/cjcp1512258 ©2016 Chinese Physical Society